Journal of Microbiology (2019) Vol. 57, No. 9, pp. 781–794
DOI 10.1007/s12275-019-9330-1
eISSN 1976-3794
pISSN 1225-8873

# Transcriptome analysis to understand the effects of the toxoflavin and tropolone produced by phytopathogenic *Burkholderia* on *Escherichia coli*[§]

**Jungwook Park[1,2†], Hyun-Hee Lee[1†], Hyejung Jung[1†], and Young-Su Seo[1*]**

[1]*Department of Microbiology, Pusan National University, Busan 46241, Republic of Korea*
[2]*Bioinformation Technology Division, Nakdonggang National Institute of Biological Resources (NNIBR), Sangju 37242, Republic of Korea*

(Received Jul 1, 2019 / Revised Jul 18, 2019 / Accepted Jul 25, 2019)

**The phytopathogenic *Burkholderia* species *B. glumae* and *B. plantarii* are the causal agents of bacterial wilt, grain rot, and seedling blight, which threaten the rice industry globally. Toxoflavin and tropolone are produced by these phytopathogens and are considered the most hostile biohazards with a broad spectrum of target organisms. However, despite their nonspecific toxicity, the effects of toxoflavin and tropolone on bacteria remain unknown. RNA-seq based transcriptome analysis was employed to determine the genome-wide expression patterns under phytotoxin treatment. Expression of 2327 and 830 genes was differentially changed by toxoflavin and tropolone, respectively. Enriched biological pathways reflected the down-regulation of oxidative phosphorylation and ribosome function, beginning with the inhibition of membrane biosynthesis and nitrogen metabolism under oxidative stress or iron starvation. Conversely, several systems such as bacterial chemotaxis, flagellar assembly, biofilm formation, and sulfur/taurine transporters were highly expressed as countermeasures against the phytotoxins. In addition, our findings revealed that three hub genes commonly induced by both phytotoxins function as the siderophore enterobactin, an iron-chelator. Our study provides new insights into the effects of phytotoxins on bacteria for better understanding of the interactions between phytopathogens and other microorganisms. These data will also be applied as a valuable source in subsequent applications against phytotoxins, the major virulence factor.**

***Keywords***: transcriptome, toxoflavin, tropolone, phytopathogenic *Burkholderia*, *Escherichia coli*

## Introduction

*Burkholderia* species comprise a vast group of Gram-negative bacteria that occupy a wide range of ecological niches (Coenye and Vandamme, 2003). Although some species are free-living in soil or freshwater as environmental bacteria, most species are associated with various hosts including humans, animals, and plants (Coenye and Vandamme, 2003; Eberl and Vandamme, 2016). Details of their interactions with hosts are usually not known, but advance in the study of phytopathogens have revealed that interactions between *Burkholderia* species and their plant hosts are harmful and cause severe plant diseases (Solis *et al.*, 2006; Kim *et al.*, 2007; Lee *et al.*, 2016). Two important phytopathogenic *Burkholderia* species, *B. glumae* and *B. gladioli,* cause bacterial wilt and grain rot in many field crops, and threaten the global rice industry (Ura *et al.*, 2006; Chun *et al.*, 2009; Nandakumar *et al.*, 2009; Ham *et al.*, 2011). They are often isolated from the same infected plants or seeds (Ura *et al.*, 2006). In addition, *B. plantarii* is the causal agent of rice seedling blight, which shows typical symptoms, including chlorosis, stunting, and root growth inhibition (Azegami *et al.*, 1987; Solis *et al.*, 2006). Because these phytopathogens thrive under high temperature and humidity, the effects of climate change, such as prolonged high nighttime temperatures and frequent rainfall, have accelerated outbreaks of plant diseases caused by *Burkholderia* species (Ham *et al.*, 2011; Wang *et al.*, 2016).

The phytopathogenic *Burkholderia* species commonly employ plant-toxic secondary metabolites, phytotoxins, which contribute to their overall pathogenicity as the most critical virulence factor (Latuasan and Berends, 1961; Ferreira *et al.*, 2010). Phytotoxins are small molecules, including alkaloids, terpenes, and especially phenolics and serve as poisonous mediators, which interfere with or sometimes kill the plant cells with the development of symptoms (Durbin, 1991; Hogenhout *et al.*, 2009). The modes of action of phytotoxins against plant hosts have been intensively studied and well characterized. Among phytotoxins, toxoflavin and tropolone are considered to be the most hostile biohazards for plant pathology. In the stationary phase, *B. glumae* and *B. gladioli* have a yellow colouring phenotype derived from toxoflavin (1,6-dimethylpyrimido[5,4-*e*]-1,2,4-triazine-5,7[1*H*,6*H*]-dione) (Jeong *et al.*, 2003; Lee *et al.*, 2016). As a very effective electron carrier between NADH and oxygen, toxoflavin generates reactive oxygen species (ROS) in the presence of oxygen and light (Latuasan and Berends, 1961; Jeong *et al.*, 2003). Effects mediated by toxoflavin cause chlorotic damage to rice panicles and inhibit the development of both leaves

[†]These authors contributed equally to this work.
*For correspondence. E-mail: yseo2011@pusan.ac.kr; Tel.: +82-51-510-2267; Fax: +82-51-514-1778
[§]Supplemental material for this article may be found at http://www.springerlink.com/content/120956.

and roots of plant hosts (Suzuki *et al.*, 1998; Yoneyama *et al.*, 1998). On the other hand, tropolone (2-Hydroxy-2,4,6-cycloheptatrien-1-one) is mainly produced by *B. plantarii* (Miwa *et al.*, 2016). Toxicity of tropolone has been attributed to its ability to function as a potent cationic metal-chelator, which contributes to its virulence and the symptoms related to seedling blight (Azegami *et al.*, 1988). When tropolone accumulates in the surrounding environment, it can also trigger the production of extracellular polysaccharides, another virulence factor, by *B. plantarii* (Wang *et al.*, 2013). Accordingly, the presence of toxoflavin and tropolone is strongly associated with yield losses in a wide spectrum of field crops (Bentley, 2008; Choi *et al.*, 2013). Moreover, since the treatment with these phytotoxins themselves leads to serious plant diseases, their mechanisms of action are of growing interest.

Despite this interest, few studies have been conducted on the interactions between phytotoxins and microorganisms. Toxoflavin and tropolone are host-nonspecific phytotoxins that affect the diverse bacteria and fungi in the environment, as well as plant hosts. Many studies have revealed that the plant microbiome plays major roles in plant growth, development, stress resistance through alteration of nutrients in plant cells and exchange of chemical signals (Lareen *et al.*, 2016; Antoniou *et al.*, 2017; Qiao *et al.*, 2017). Therefore, research into the effects of phytotoxins on bacteria will be a valuable source of information on what has been called the plant's second genome. Until now, there are some reports that treatment of toxoflavin and tropolone inhibits the growth of bacteria (Latuasan and Berends, 1961; Trust, 1975). In 1975, it was demonstrated that 0.5–2.5 μg/ml concentrations of toxoflavin directly inhibited the growth of genera *Escherichia*, *Shigella*, *Micrococcus*, and *Bacillus* (Latuasan and Berends, 1961). Tropolone was also shown to be strong antibacterial activity for a wide range of gram-negative and gram-positive bacterial species (Trust, 1975). However, the detailed mechanism of toxoflavin and tropolone phytotoxins to inhibit bacterial growth is still unknown. The molecular network by two phytotoxins in bacteria could be applied as a reference guide for future research.

In the present study, we investigated the effects of toxoflavin and tropolone from phytopathogenic *Burkholderia* species on bacteria using transcriptome analysis. Our study aimed to characterize the features of genes differentially expressed during treatment with the phytotoxins compared with the methanol control. To this end, we constructed RNA-seq libraries of *Escherichia coli* K-12 MG1655, as a model bacterium, under each minimal inhibitory concentration (MIC) of toxoflavin and tropolone. The COG protein families and KEGG pathway database were used to understand biological systems of the expressed genes. We also focused on determining the hub genes that are induced in both phytotoxin stress conditions, using network analysis with the STRING database. Our work will provide new insights into the effects of phytotoxins on bacteria and improve our understanding of the interactions between phytopathogenic bacteria and other microorganisms.

## Materials and Methods

### Bacterial strain, culture conditions, and chemicals

In this study, *E. coli* K-12 MG1655 was used and stored at -80°C in 30% glycerol for a long-term preservation. To isolate a single colony of this bacterium, the stock was streaked onto Luria Bertani (LB; Difco) media supplemented with 15 g/L Bacto agar (Difco) and then incubated overnight 37°C. A single colony on the LB agar plate was aerobically cultured in LB liquid at 37°C with constant shaking. Toxoflavin and tropolone were purchased from Sigma-Aldrich as synthetic chemicals with ≥ 98% purity. These phytotoxins were dissolved in methanol as a solvent.

### Minimal inhibitory concentration (MIC) test

A MIC test was carried out by using a standard micro-dilution method (Yang *et al.*, 2014). Different concentrations of toxoflavin and tropolone at final concentrations of 1, 10, and 100 μM were added to a 1:100 dilution of overnight cultures of *E. coli* K-12 MG1655, followed by incubation at 37°C for 10 h. To determine MIC, bacterial growth was indexed by measuring the optical density (at $\lambda$ = 600 nm) at 2 h intervals using a UV-1800 spectrophotometer (Shimadzu). The overnight cultures of *E. coli* K-12 MG1655 were subcultured in fresh LB liquid until the $OD_{600}$ value reached 0.5. 100 μl of cultures diluted $1 \times 10^{-5}$ with distilled water was spread onto LB agar plates containing toxoflavin and tropolone at the MIC. After incubation at 37°C for 12 h, bacterial colony formation was observed by the photography. LB medium and methanol were carried out in parallel and all tests were conducted as three independent replicates.

### RNA extraction and sequencing

The overnight primary cultures were diluted 1:100 to initiate the experimental cultures. When cultures reached exponential phase corresponding to $OD_{600}$ = 0.5, two cultures were mixed with toxoflavin or tropolone to yield final concentrations of 10 μM and 100 μM, respectively. The volume of methanol corresponding to each of the phytotoxin conditions was added to the cultures as control samples. After 2 h of phytotoxin exposure, each culture was harvested by centrifugation at 12,000 × *g* for 1 min at 4°C. Three biological replicates were prepared for samples of RNA-seq.

Total RNA was extracted from the harvested bacterial pellets using an RNeasy Midi kit (Qiagen). Residual genomic DNA contamination was removed with an RNase-Free DNase kit (Qiagen). rRNA depletion was then performed with a MICROB*Express*™ bacterial mRNA enrichment kit (Ambion) following the manufacturer's instructions. The concentrations and 260/280 ratios of enriched mRNAs were determined using a NanoDrop 2000 (Thermo scientific). Subsequently, RNA-seq libraries were prepared using an Illumina TruSeq™ RNA sample prep kit (Illumina) with a standard low-throughput protocol. Paired end sequencing using an Illumina HiSeq-2000 platform was conducted at the national instrumentation center for environmental management (Nicem).

### RNA-seq analysis

The FASTX-Toolkit filtered out low-quality reads by a Phred score (50% of sequence ≥28 quality score) (http://hannonlab.cshl.edu/fastx_toolkit/). An in-house python script was used to synchronize the forward and reverse directions of filtered reads. Paired reads were aligned to a reference genome (NCBI accession no. GCF_000005845.2) of *E. coli* K-12 MG1655 using the BWA-MEM module (Li and Durbin, 2009). SAMtools converted the mapping results derived from the BWA to binary format BAM files, and then sorted them by chromosomal coordinates (Li *et al.*, 2009). The number of mapping reads that aligned to all CDSs in *E. coli* K-12 MG1655 were tabulated using the FeatureCounts tool in the Subread package (Liao *et al.*, 2014).

### DEGs analysis

For the statistical analysis, the counting reads of each CDS were used as an input data. Differential expression analysis was performed using an EdgeR package in the R statistical environment, which employs a negative binomial distribution method (Robinson and Smyth, 2008; Robinson *et al.*, 2010). For EdgeR analysis, a trimmed mean of the M-values (where M = $\log_2$-fold change) method and a quantile-adjusted conditional maximum likelihood method were used to calculate the normalization factor and expression differences for estimating dispersions, respectively (Robinson and Smyth, 2008; Robinson *et al.*, 2010). *P*-values were adjusted for multiple testing with the Benjamini-Hochberg procedure as a false discovery rate (FDR) value (Benjamini and Hochberg, 1995). Afterwards, we explored the effects of phytotoxins on gene expression compared to the methanol controls. Significant difference in expressions were determined using two criteria: $|\log_2\text{-fold change}| \geq 1$ and FDR $< 0.05$. These analyses were performed independently in toxoflavin and tropolone using the same control data.

### COG analysis for common DEGs

The lists of DEGs derived from the toxoflavin and tropolone conditions were compared to identify core groups commonly affected by both phytotoxins. COG functional categories for common DEGs were downloaded from the NCBI COG database (Galperin *et al.*, 2015). The DIAMOND tool was applied to align the amino acid sequences against the COG database with following parameters: *e*-value = $1 \times 10^{-5}$; identity = 30%; coverage = 30% (Buchfink *et al.*, 2015). The description of best hit (with lowest statistical *e*-value) was assigned as the annotation of common DEGs. The COG IDs of all annotations were then classified based on their COG categories.

### KEGG pathway enrichment analysis

Pathway information from the KEGG database (https://www.genome.jp/kegg/) was used to investigate the response of biological systems to the phytotoxins. To accomplish this, we downloaded a molecular interaction/reaction network for *E. coli* K-12 MG1655 listed in KEGG database, and each pathway was matched to DEGs via an in-house python script. Significant enrichment was identified using a hypergeometric test with the phyper function contained in the R statistical environment (Qureshi and Sacan, 2013). The hypergeometric test considered the following statistics: the number of all genes involved in KEGG systems; the percentage of the KEGG systems covered by specific pathway; expected number of DEGs in the specific pathway. We selected the pathways with a *p*-value < 0.05 as significant enriched. A molecular network map within the pathways was constructed by Cytoscape tool (https://cytoscape.org/).

### Interaction network from STRING

Interaction network of co-up-regulated DEGs from each group comparison (toxoflavin vs. control and tropolone vs.

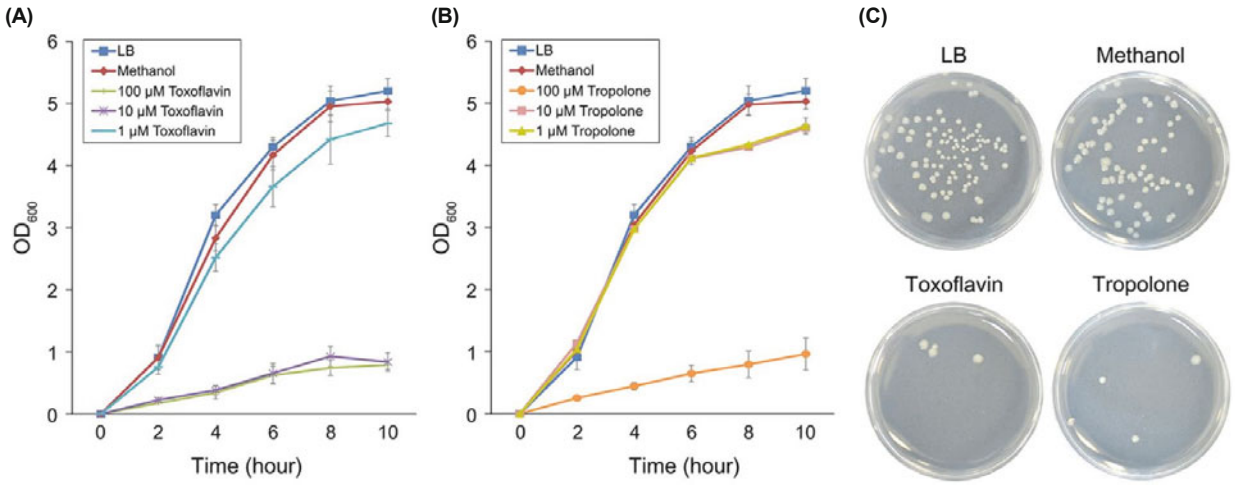


**Fig. 1. Growth pattern of *E. coli* K-12 MG1655 in treatment of toxoflavin and tropolone. (A) Growth curves of bacteria exposed to the following concentrations of toxoflavin: 1 μM, 10 μM, and 100 μM.** (B) Growth curves of bacteria exposed to the following concentrations of tropolone: 1 μM, 10 μM, and 100 μM. Bacterial growth was monitored by measuring the absorbance 600 nm at intervals of 2 h. The LB medium and methanol solvent were used in parallel. All growth curves with the standard deviation resulted from three replicates for each treatment. (C) Colony formation of bacteria on LB plates with phytotoxins. After the culture was streaked with *E. coli* K-12 MG1655, the plates were incubated for 12 h at 37°C.

control) was analyzed by the STRING database, which is a database for searching for known and predicted interactions (Szklarczyk *et al.*, 2017). The interactions are established based on published literature describing experimentally studied interactions, as well as those from genome analysis. These sources include neighborhood, gene fusion, co-occurrence, co-expression, experiments, databases, and text-mining. To minimize false positives as well as false negatives, some interactions considered low-confidence (less than 0.4 score) were eliminated in this study. Within network, highly interconnected genes with other co-up-regulated DEGs were considered as the hub genes.

### Nucleotide sequence accession number

All raw data have been submitted to the NCBI GEO database under accession number GSE133348.

## Results and Discussion

### Antibacterial activity of toxoflavin and tropolone against *E. coli* K-12 MG1655

*E. coli* is one of the most widely studied model organisms, which has been intensively investigated for over 60 years. Laboratory strains derived from wild-type *E. coli* have been used as versatile tools of molecular biology, due to its fast growth, relative cheap culture media, and industrial scalability (Blount, 2015; Fathima and Rao, 2018). Since the whole-genome sequencing of *E. coli* K-12 MG1655 (Blattner *et al.*, 1997), global studies have been dedicated to generating extensive knowledge on its transcriptome, proteome, and metabolome (Champion *et al.*, 2003; Franchini and Egli, 2006; McCloskey *et al.*, 2014; Fathima and Rao, 2018). Thereby this strain has the most comprehensive and functional sets of resources on various public databases (McIntosh *et al.*, 2012; Keseler *et al.*, 2013; Zhou *et al.*, 2013; Hu *et al.*, 2014). Therefore, we selected *E. coli* K-12 MG1655 as a bacterial standard model against phytotoxins.

To investigate the MIC with toxoflavin and tropolone, we monitored the bacterial growth curve in *E. coli* K-12 MG1655. As shown in Fig. 1A and B, these phytoxins inhibited bacterial growth in a concentration-dependent manner. At the concentration of 10 μM (MIC), toxoflavin completely suppressed the growth of *E. coli*, whereas tropolone had a MIC = 100 μM. The addition of only methanol did not affect the growth pattern as did the result in LB medium. In addition, numerous *E. coli* colonies were observed on the LB and methanol plates in the bacterial colony formation assay (Fig. 1C). Our results indicated that two phytotoxins have antibacterial activity against *E. coli* and the treatment with toxoflavin reduced bacterial growth more severely than that of tropolone. The MIC of toxoflavin and tropolone were selected to treat *E. coli* K-12 MG1655 for the following transcriptome analysis with RNA-seq.

### Summary of RNA-seq data sets

To gain insight into the genome-wide transcriptional patterns in the presence of the phytotoxins, we conducted RNA-seq analysis for *E. coli* K-12 MG1655. RNAs were isolated from bacteria harvested at the exponential phase ($OD_{600}$ = 0.5) with toxoflavin (a final concentration of 10 μM) or tropolone (100 μM) (Supplementary data Table S1). After sequencing the transcriptome on Illumina HiSeq2000 platform, nine libraries including the phytotoxins and the methanol control yielded a total of 13,575,232 to 62,764,318 reads of 126 bp in length (Table 1). The total length of the reads was about 36.9 Gbp, representing a more than 7900-fold coverage of the *E. coli* K-12 MG1655 genome. The Phred scores of the raw reads in each library showed their high quality with an average value of 36 (Supplementary data Fig. S1). The value defined as '$-10 \times \log(probability)$' is a critical component for predicting the probability of base-call errors (Ewing and Green, 1998; Richardson *et al.*, 2007); *e.g.* a Phred score of 30 value corresponds to one error in every 1000 base-calls, or 99.9% accuracy. To profile the gene expression, filtered reads from the nine libraries were aligned onto the reference genome of *E. coli* K-12 MG1655. The 4.64 Mbp single genomic replicon carries a total of 4566 genes, of which 4242 are CDSs, which have a 50.8% G+C content (Riley *et al.*, 2006). The BWA tool produced good mapping results, ranging from 90.0% (12,218,654 reads) to 97.7% (28,442,271 reads) (Supplementary data Table S2). Indeed, when the sequencing depth in *E. coli* reaches around 13 million reads, most genes with an RPKM (reads per kilobase of a gene per million reads) value of 1 or more are detected (Mortazavi *et al.*, 2008; Haas *et al.*, 2012). Additional depth beyond this point did not contribute much in increasing the percentage of genes detected by RNA-seq (Haas *et al.*, 2012). Thus, considering the high Phred score and mapping results, our RNA-seq datasets had the sufficient accuracy and coverage for downstream analyses of the transcriptome.

**Table 1.** Overview of RNA-seq data

| Sample | Read type | Length | GC (%) | Phred score | Total reads |
|---|---|---|---|---|---|
| Control_1 | Paired end | 126 | 52 | 36 | 29,101,600 |
| Control_2 | Paired end | 126 | 52 | 36 | 62,764,318 |
| Control_3 | Paired end | 126 | 52 | 36 | 46,639,630 |
| Toxoflavin_1 | Paired end | 126 | 53 | 36 | 21,950,224 |
| Toxoflavin_2 | Paired end | 126 | 53 | 36 | 24,176,494 |
| Toxoflavin_3 | Paired end | 126 | 53 | 36 | 37,771,312 |
| Tropolone_1 | Paired end | 126 | 53 | 36 | 30,921,910 |
| Tropolone_2 | Paired end | 126 | 52 | 36 | 25,733,234 |
| Tropolone_3 | Paired end | 126 | 52 | 36 | 13,575,232 |

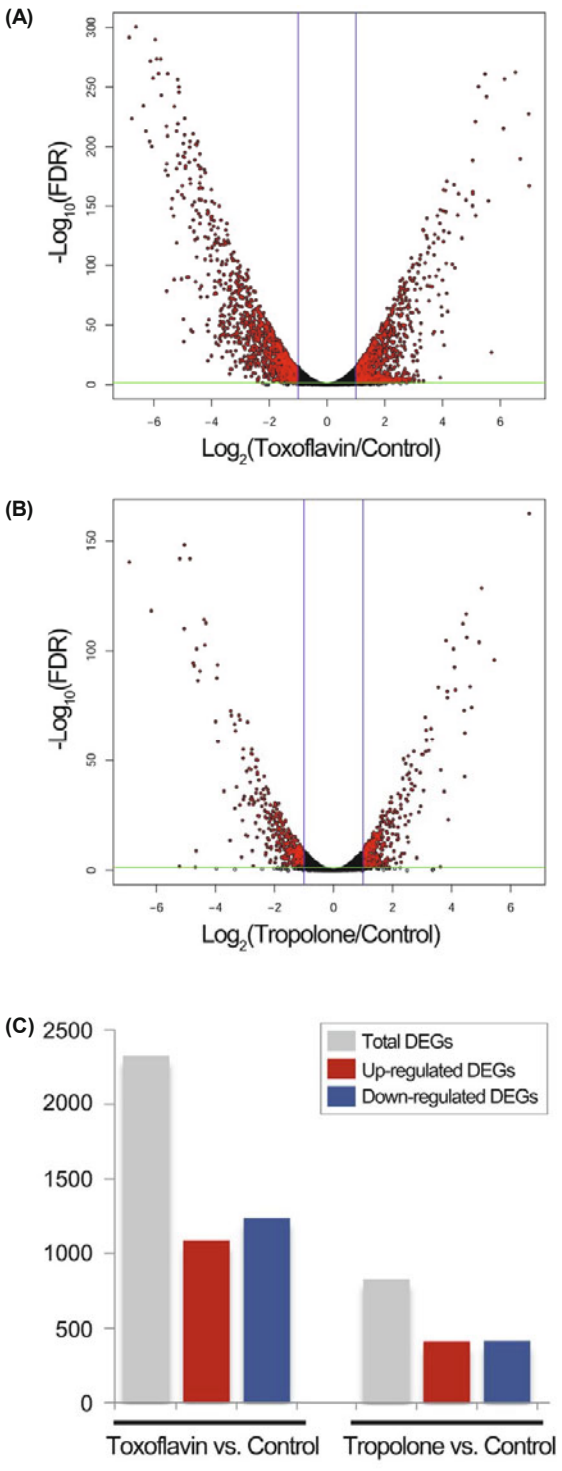


**Fig. 2. Overview of the DEGs induced by phototoxins.** (A) Volcano plot of DEGs between toxoflavin and control. (B) Volcano plot of DEGs between tropolone and control. The differential expression analysis was performed by the EdgeR statistical package. In plots, circle points indicate each gene of *E. coli* K-12 MG1655. Two criteria of |fold change| ≥ 2 and false discovery rate (FDR) < 0.05 were highlighted in blue and green lines, respectively. The red points mean significantly up-regulated or down-regulated DEGs. (C) Distribution of DEGs. The bar graphs indicate distribution of DEGs under each phytotoxin condition. The red and blue colored bars are numbers of up-regulated and down-regulated DEGs, respectively.

### Comparative gene expression analysis under phytotoxin conditions

Nine RNA-seq libraries were visualized in two dimensions using multidimensional scaling of EdgeR (Robinson *et al.*, 2010), which revealed that each dataset (the phytotoxins toxoflavin and tropolone and the controls) was distinctively labeled (Supplementary data Fig. S2). The total number of DEGs induced by the phytotoxins is listed in Supplementary data Table S3. Comparison of toxoflavin to control conditions identified 2327 differentially expressed genes (DEGs) (Fig. 2A). Of these DEGs, 1088 genes were significantly up-regulated and 1239 genes were significantly down-regulated (Fig. 2C). In contrast, there were only 830 DEGs in the tropolone treatment with 413 up-regulated DEGs and 417 down-regulated DEGs (Fig. 2B and C). In general, many DEGs have been detected through transcriptome analysis in studies on bacterial interactions with harsh conditions such as *in vivo* environment, nutrient starvation, and abiotic stress (Jacobs *et al.*, 2012; Kim *et al.*, 2014; Liu *et al.*, 2014, 2017; Choi *et al.*, 2016). In rice-pathogenic *B. glumae* BGR1, the *in vivo* environment with its diverse stresses causes overwhelming effects (> 2000 DEGs) on genome-wide transcription involved in a variety of metabolic and signaling pathways (Kim *et al.*, 2014). The distribution of DEGs suggested that the antibiotic activity of toxoflavin has greater effects on the physiology of bacteria than that of tropolone. These results were consistent with the bacterial growth curves when exposed to the phytotoxins (Fig. 1).

To better understand the global bacterial responses to phytotoxins, we performed a comparative analysis between the DEGs in the toxoflavin and tropolone conditions (Fig. 3). Common DEGs were classified through homology with protein functions determined from the COG database. COG analysis assigned 312 co-down-regulated DEGs to 22 functional categories, most of which belonged to the following terms: energy production and conversion (C, 16.4%), translation, ribosomal structure and biogenesis (J, 14.2%), and amino acid transport and metabolism (E, 10.9%) (Fig. 3A). Given that the biosynthesis of cellular energy and functional proteins is an absolute requirement for living organisms, toxoflavin and tropolone would have severely inhibited bacterial growth by directly or indirectly targeting genes associated with these biosynthetic systems. Membrane biogenesis also appears to be a particularly effective target for toxins. Our COG analysis showed 24 co-down-regulated DEGs associated with cell wall/membrane/envelope biogenesis (M, 7.3%) (Fig. 3A). Several phytotoxins can damage the cellular membrane in plants (Heiser *et al.*, 1998; Möbius and Hertweck, 2009). They not only cause major damage to membrane lipids through ROS, but also hamper membrane biosynthesis resulting in a perturbed membrane ordering and increased membrane permeability (Heiser *et al.*, 1998; Fry and Loria, 2002; Williams *et al.*, 2007). Bischoff *et al.* (2009) revealed that treatment with phytotoxin thaxtomin A alters the transcriptional expression of genes involved in primary and secondary cellulose synthesis and pectin metabolism, which affects the deposition or composition of plant cell walls. Although the composition and biosynthesis of the membrane differs from plant cell walls, the toxicity of toxoflavin and tropolone would have caused critical damage to

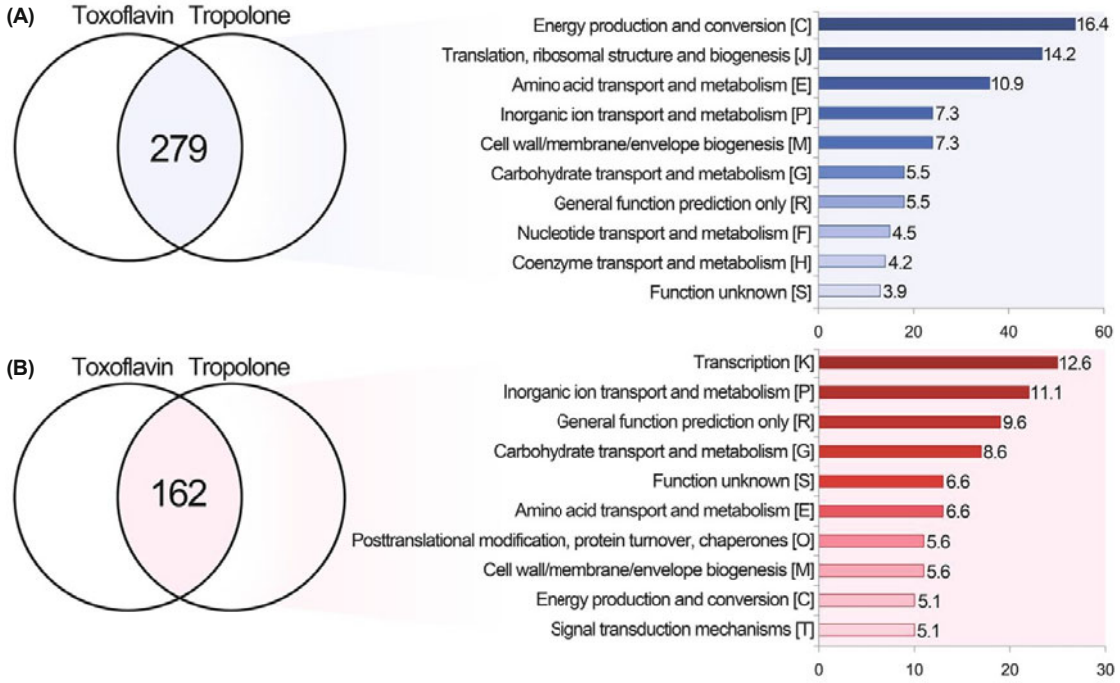


**Fig. 3. The identification of common DEGs in phytotoxins.** Venn diagrams that show the common DEGs between toxoflavin and tropolone conditions: co-up-regulated DEGs (A) and co-down-regulated DEGs (B). The top 10 COG functional categories of common DEGs are illustrated. The length of the bars represents the number of genes in each COG. The percent assigned to each COG refers to the coverage of the total number in the common DEGs accounted for in the model. Some common DEGs have multiple COG category assignments.

the bacterial membrane. Since the multilayer membrane protects itself from various biotic and abiotic stresses, exact biogenesis of membrane is crucial for the survival of bacteria (Ruiz *et al.*, 2006; Delcour, 2009). Defects in membrane functionality can cause bacteria to be outcompeted by the surrounding microorganisms, as well as attenuating of the ability to infect the host (Kuehn and Kesty, 2005; Ieva, 2017).

A total of 213 co-up-regulated DEGs were found in both toxoflavin and tropolone conditions (Fig. 3B). Bacteria would need countermeasure strategies against the stress conditions caused by phytotoxins. Within the COG-assigned categories, the largest number of co-up-regulated DEGs were involved in the transcription (K, 12.6%), consisting of diverse transcriptional regulators (Fig. 3B). In response to environmental cues, including biotic/abiotic stresses, bacteria detect signals from membrane-bound sensor proteins and activate the transcriptional regulator, which initiates the corresponding cellular responses (Parkinson and Kofoid, 1992; Hoch, 2000; Krämer, 2010). According to the current view, we observed a high incidence (10 DEGs, 5.1%) of co-up-regulation for functions involved in signal transduction mechanisms (T) (Fig. 3B). Although the COG database with broad functional categories could not provide details of each biological system, inorganic ion transport and metabolism (P, 11.1%), where the second largest number of co-up-regulated DEGs were distributed, is expected to be one of the essential cellular responses to phytotoxins (Fig. 3B). We suggest that, like plant ion transporters, bacterial ion transporters have enormous potential to affect stress tolerance to phytotoxins (Blumwald, 2000; Maathuis, 2007; Brini and Masmoudi, 2012).

## Biological systems down-regulated by toxoflavin and tropolone

To investigate which biological systems were differentially regulated by toxoflavin and tropolone, we found the KEGG pathways for the DEGs for each phytotoxin. Of the 2327 DEGs derived from the toxoflavin condition, 868 DEGs were matched to 116 pathways. In the tropolone condition, 314 of the 830 DEGs were matched to 92 pathways. Enrichment

**Table 2. Enriched pathways of down-regulated DEGs induced by toxoflavin**

| KEGG ID | Pathway | Count | *p*-value[a] |
|---|---|---|---|
| eco00190 | Oxidative phosphorylation | 38 | 7.2E-12 |
| eco03010 | Ribosome | 52 | 1.8E-07 |
| eco01110 | Biosynthesis of secondary metabolites | 148 | 2.7E-05 |
| eco00250 | Alanine, aspartate and glutamate metabolism | 23 | 0.0002 |
| eco01501 | beta-Lactam resistance | 14 | 0.0002 |
| eco01100 | Metabolic pathways | 370 | 0.0003 |
| eco01130 | Biosynthesis of antibiotics | 102 | 0.0007 |
| eco00061 | Fatty acid biosynthesis | 11 | 0.0008 |
| eco01230 | Biosynthesis of amino acids | 60 | 0.0020 |
| eco00540 | Lipopolysaccharide biosynthesis | 23 | 0.0025 |
| eco00340 | Histidine metabolism | 7 | 0.0063 |
| eco00620 | Pyruvate metabolism | 28 | 0.0200 |
| eco00020 | Citrate cycle (TCA cycle) | 16 | 0.0208 |
| eco01120 | Microbial metabolism in diverse environments | 116 | 0.0262 |
| eco00430 | Taurine and hypotaurine metabolism | 5 | 0.0332 |
| eco01502 | Vancomycin resistance | 6 | 0.0394 |

[a]The statistical significance calculated by hypergeometric test.

**Table 3. Enriched pathways of down-regulated DEGs induced by tropolone**

| KEGG ID | Pathway | Count | *p*-value[a] |
|---|---|---|---|
| eco03010 | Ribosome | 34 | 7.8E-13 |
| eco00190 | Oxidative phosphorylation | 23 | 3.1E-11 |
| eco00910 | Nitrogen metabolism | 11 | 4.0E-05 |
| eco00250 | Alanine, aspartate, and glutamate metabolism | 12 | 0.0003 |
| eco01501 | β-Lactam resistance | 8 | 0.0004 |
| eco00633 | Nitrotoluene degradation | 4 | 0.0055 |
| eco02020 | Two-component system | 27 | 0.0242 |

[a] The statistical significance calculated by hypergeometric test.

analysis was subsequently conducted to identify the significantly induced pathways with $p$-value <0.05. The largest number of down-regulated DEGs common to both toxoflavin and tropolone, were enriched in oxidative phosphorylation (eco00190) and ribosome (eco03010) (Tables 2 and 3), which coincided with the results of COG analysis (Fig. 3). Toxoflavin significantly inhibited the expression of 52 genes (an average $\log_2$-fold change = −4.24) related to large and small subunits of ribosome, especially the 30S ribosomal subunit protein S10 (b3321), which showed a 115-fold decrease compared to the control (Supplementary data Table S4). The core oxidative phosphorylation modules of NADH dehydrogenase, succinate dehydrogenase, cytochrome *c* oxidase, the F-type ATPase and cytochrome *bd* complex were down-regulated by toxoflavin between −2.50 and −27.28-fold (Supplementary data Table S4).

However, the enriched pathways other than oxidative phosphorylation and the ribosome had different specificities for each phytotoxin. Comparing toxoflavin and control, showed that down-regulated DEGs were significantly enriched in fatty acid biosynthesis (eco00061, 11 DEGs), lipopolysaccharide biosynthesis (eco00540, 23 DEGs), citrate cycle (TCA cycle) (eco00020, 16 DEGs) and many metabolism systems (63 DEGs) such as eco00250 (for alanine, aspartate and glutamate), eco00340 (histidine), eco00620 (pyruvate), and eco00430 (taurine and hypotaurine) (Table 2). Surprisingly, we found that these down-regulated pathways were placed in a damage reaction cascade mediated by toxoflavin (Fig. 4A). The ROS generated by toxoflavin induce the production of superoxides ($O_2^-$) and hydrogen peroxide ($H_2O_2$) (Latuasan and Berends, 1961; Ham *et al.*, 2011). Because of the high reactivity from free radicals, these ROS damage three major classes of biological molecules including nucleic acids, proteins, and lipids (Dröge, 2002; Phaniendra *et al.*, 2015; Jung *et al.*, 2018). In *in situ* environment with many competitors, the bacterial membrane will be the front line confronted with the reactivity and toxicity of ROS. We have already identified the co-down-regulated DEGs in cell wall/membrane/envelope biogenesis via COG analysis (Fig. 3), where the down-regulation of fatty acid biosynthesis and lipopolysaccharide biosynthesis was considered as a major cause (Table 2). Toxoflavin can directly attack polyunsaturated fatty acids in bacterial membrane to induce lipid peroxidation (Ham *et al.*, 2011; Kashef and Hamblin, 2017). It was reported that the lipid peroxidation alters the composition and integrity of membrane, which lead to a loss of function of membrane-bound proteins, *e.g.* the oxidative phos-

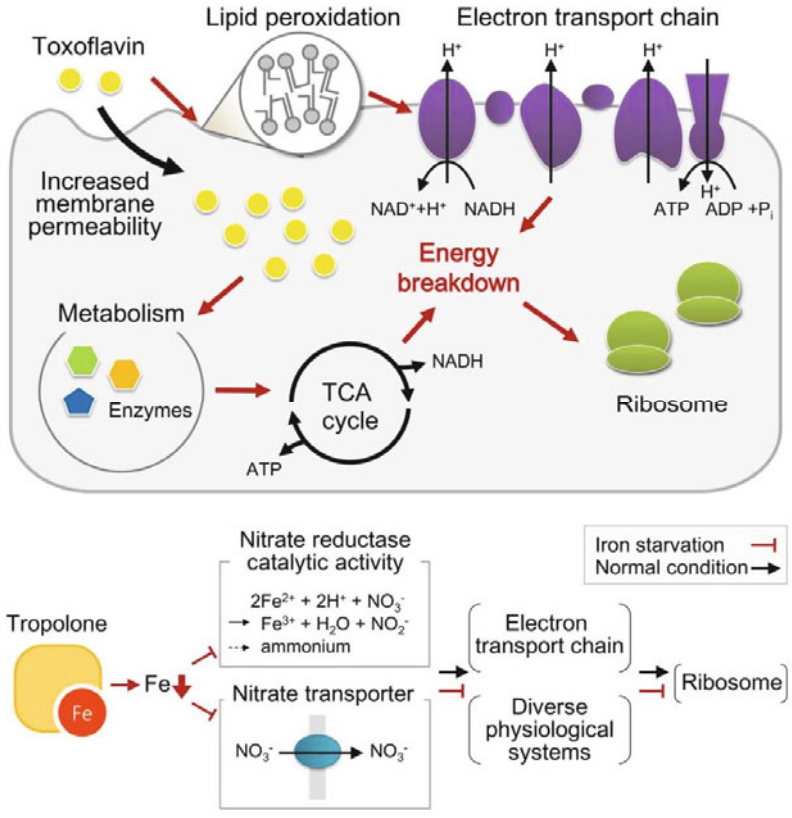


**Fig. 4. Schematic hypothetical model of phytotoxin-induced bacterial death.** (A) Oxidative stress induced by toxoflavin phytotoxin. Bacterial membrane composed of lipids is damaged by toxoflavin with oxidative stress, which induces lipid peroxidation. The lipid peroxidation leads to a loss of function of membrane-bound proteins for oxidative phosphorylation. Toxoflavin introduced into the bacterial cell targets enzyme proteins associated with diverse metabolism. Disability of oxidative phosphorylation and TCA cycle results in inhibition of the synthesis of ATP, a cellular energy source. Finally, an energy breakdown influences on ribosome organization for functional protein biosynthesis underlying a crucial cause of bacterial death. (B) Iron starvation induced by tropolone phytotoxin. Bacteria are exposed to an iron-starved stress in the presence of tropolone, a highly active iron-chelator. In nitrogen metabolism, nitrate reductase and transporter that use iron ions as the cofactor are inhibited. The problem of nitrogen source synthesis has a negative effect on diverse physiological systems. The nitrogen reductase inhibited by a loss of iron ions does not terminate oxidative phosphorylation in electron transport chains. Similar to the effects in toxoflavin, disability of these systems suppresses the ribosome function.

phorylation of electron transport chain (Farr and Kogoma, 1991). Furthermore, following lipid peroxidation, increased membrane permeability would accelerate the influx of toxoflavin phytotoxin. The toxoflavin within bacterial cells targets enzyme proteins associated with a variety of metabolic processes, disrupting the TCA cycle (Table 2). Consequently, an energy breakdown in oxidative phosphorylation and the TCA cycle would contribute to the loss of ribosome organization for functional protein biosynthesis underlying a crucial cause of bacterial death (Table 2). Recently, Willi *et al.* (2018) demonstrated that the damaged 23S rRNA by ROS *in vivo* critically inhibits the ribosome function during protein biosynthesis.

On the other hand, the following five systems were down-regulated in the tropolone condition: nitrogen metabolism (eco00910), 11 DEGs; alanine, aspartate and glutamate metabolism (eco00250), 12 DEGs; beta-lactam resistance (eco01501), 8 DEGs; nitrotoluene degradation (eco00633), 4 DEGs; two-component system (eco02020), 27 DEGs (Table 3). If toxoflavin causes a damage reaction cascade from membrane damage to bacterial death by energy breakdown (Fig. 4A), treatment with tropolone was responsible for a decrease in bacterial growth by inducing starvation stress (Fig. 4B). Tropolone functions as a highly active iron-chelator, like as a siderophore molecule, for its broad-spectrum antimicrobial activity against bacteria and fungi (Wakimoto *et al.*, 1986; Azegami *et al.*, 1988). Bacteria will experience iron starvation in the presence of tropolone secreted by *B. plantarii*. We noticed that most down-regulated DEGs in nitrogen metabolism are intensively distributed on the reductases (*e.g.* b1224, $\log_2$-fold change = −4.32; b1225, −3.17; b1227, −1.81; b1465, −1.70; b1467, −1.77; b1468, −1.76; b2203, −1.12; b2206, −1.78) and transporter (*e.g.* b1223, $\log_2$-fold change = −1.83; b1469, −1.24) for nitrate (Table 3 and Supplementary data Table S4). It has been reported that iron sulfur compounds serve as essential cofactors in the reductase from nitrate ($NO_3^-$) via nitrite ($NO_2^-$) to ammonium ($NH_4^+$) (Morozkina and Zvyagilskaya, 2007; Allen *et al.*, 2008; Jing *et al.*, 2019). Several studies have demonstrated that these genes are down-regulated at the expression levels by iron-limited conditions (Timmermans *et al.*, 1994; Allen *et al.*, 2008). Our results also support the importance of interactions between nitrogen metabolism and iron nutrients. Since nitrogen sources are required for all the key constituents of the cell, including amino

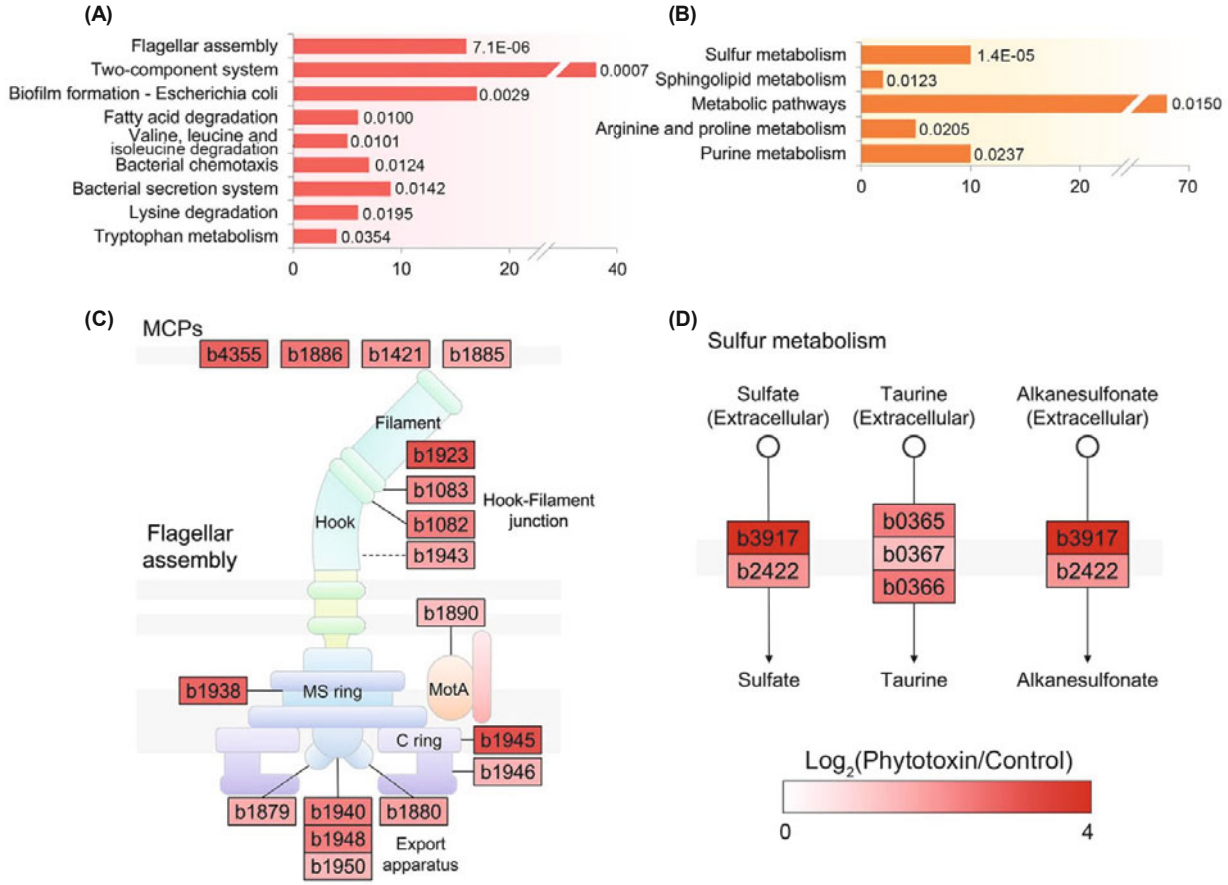


**Fig. 5. KEGG pathway analysis of up-regulated DEGs.** (A) Enriched pathways under toxoflavin condition. (B) Enriched pathways under tropolone condition. Enrichment analysis was performed by hypergeometric test with a significant criterion, $p$-value < 0.05. For each KEGG pathway, the bar shows the number of enriched genes. (C) Bacterial chemotaxis and flagellar assembly highly induced by toxoflavin phytotoxin. (D) Sulfur metabolism highly induced by tropolone phytotoxin. Molecular network of representative enriched pathways was constructed by the Cytoscape tool. There are two node types: rectangle type, protein; circle type, biological chemical. Color variation from white to red represent $\log_2$ (Phytotoxin/Control) values from a minimum of 0 to a maximum of 4. In color variation, the 0 point indicates the same expression level between phytotoxin and control conditions.

acids, pyrimidines and purines, NAD, and amino sugar in gram-negative bacteria (Reitzer, 1987, 2003), nitrogen metabolism has a huge impact on diverse physiological systems. Therefore, considering that membrane-bound nitrogen reductases plays an important role in terminating respiratory electron transport chains (Simon *et al.*, 2003), the disruption of the nitrogen metabolism could well explain the down-regulation of ribosome (34 DEGs) and oxidative phosphorylation (23 DEGs) induced by tropolone (Table 3 and Fig. 4B).

**Biological systems up-regulated by toxoflavin and tropolone**

KEGG pathways enriched in up-regulated DEGs are shown in Fig. 5A and B. Bacteria seemed to select countermeasure strategies to evade and protect against ROS damage by toxoflavin (Fig. 5A). Bacterial chemotaxis (eco02030), which was enriched with seven DEGs, allows bacteria to move away from toxic substances, including toxoflavin (Fig. 5C) (Benov and Fridovich, 1996). Four genes: b1421 (2.77-fold increase), b1885 (2.35), b1886 (3.57), and b4355 (4.24) were highly up-regulated in methyl-accepting chemotaxis proteins (MCPs) for the recognition of repellents (Fig. 5C and Supplementary data Table S4). Above all, we have confirmed that up-regulated DEGs induced by toxoflavin include the flagellar assembly system (eco02040) in an almost perfect manner (16 of total 37 genes, 43.2%) to generate the driving force (Fig. 5C). Studies on genera *Pseudomonas* and *Salmonella* showed that swarming and swimming motility have a significant effect on resistance to antimicrobial compounds (Gooderham and Hancock, 2009; Ugurlu *et al.*, 2016; Amina and Ahmed,

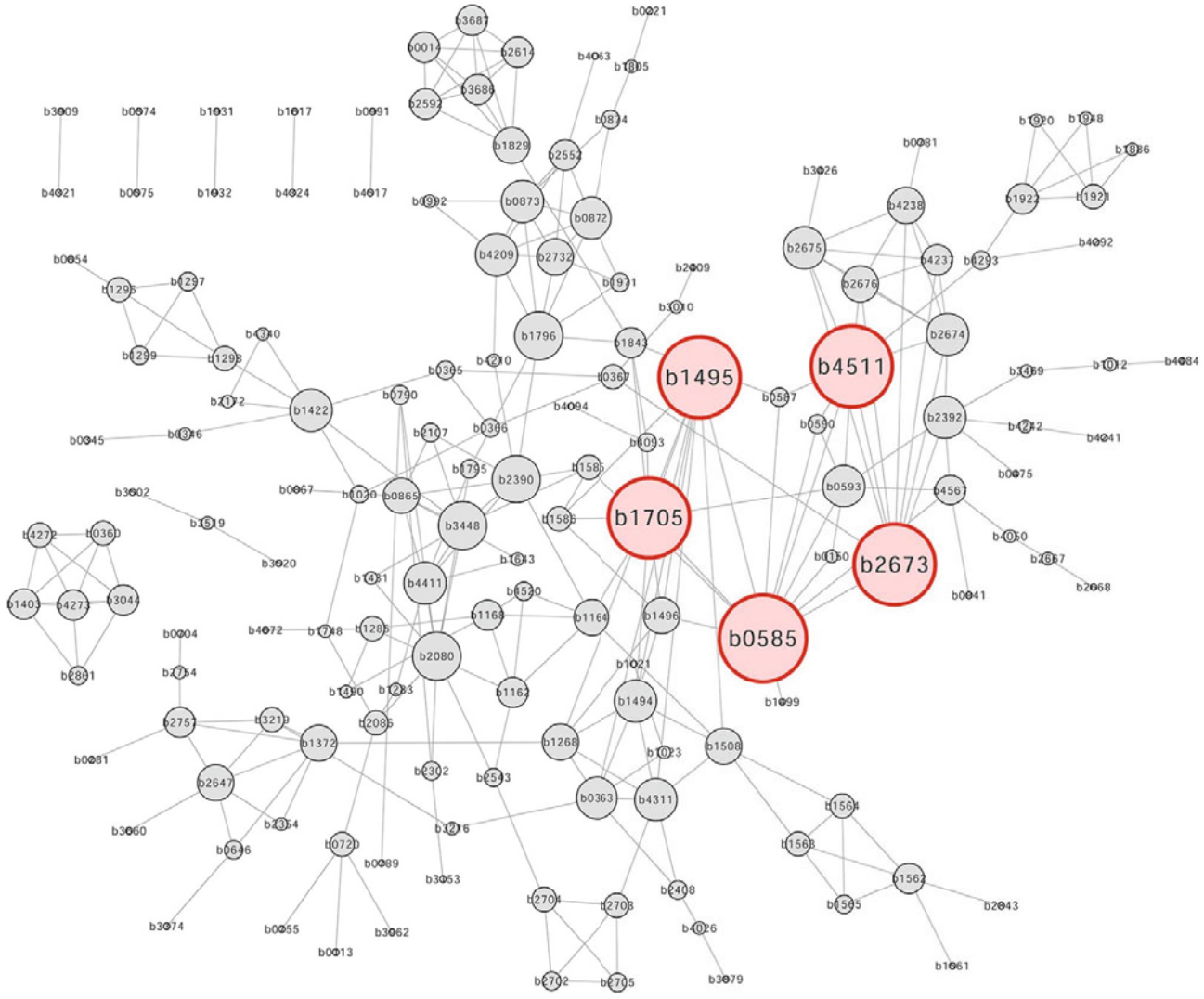


**Fig. 6. Interaction network of co-up-regulated DEGs in phytotoxin conditions.** Interactions among co-up-regulated DEGs induced by both toxoflavin and tropolone were constructed from the STRING database. The Cytoscape visualized expanded view of the network, where nodes represent co-up-regulated DEGs and edges the known or predicted interactions with a high-confidence > 0.4 score. The size of the nodes reflects the number of interactions with other genes, *i.e.* the smallest node has only one gene interaction. As hub genes, co-up-regulated DEGs with more than nine interactions are selected and highlighted in red circle.

2017). In addition to the evasion derived from the flagellar structure, biofilm formation (eco02026) was highly enriched with 17 up-regulated DEGs (Fig. 5A). As a consequence of chemical interactions, biofilm formation enhances the ability of the microbial communities to adapt to adverse conditions (Vasudevan, 2014). The extra polymeric matrices that make up biofilm would prevent the penetration of toxoflavin phytotoxin into bacterial cells. The significant enrichment (nine up-regulated DEGs) in only the type II bacterial secretion system (eco03070), which is known to secrete extracellular matrix proteins in *E. coli* (Baldi *et al.*, 2012), will also be important evidence of the essentiality of the biofilm formation against toxoflavin (Supplementary data Table S4). It was interesting that the flagellar structure and biofilm formation were highly induced in phytopathogenic *B. glumae*, when a quorum-sensing system activated the production of toxoflavin (Kim *et al.*, 2004, 2007, 2013). We hypothesized that other bacteria could mimic these evasion and protection mechanisms induced by toxoflavin of *B. glumae*.

There were a few significantly enriched systems from the up-regulated DEGs of tropolone condition, and the number of DEGs within each system was not enough (Fig. 5B). However, we observed that ten up-regulated DEGs in sulfur metabolism (eco00920) are concentrated in some functional modules, and not randomly distributed (Fig. 5D). Among these, six up-regulated DEGs in particular were involved in transporters for extracellular sulfate/taurine/alkanesulfonate as follows: b0365 for taurine ABC transporter periplasmic binding protein, 3.42-fold increase; b0366 for taurine ABC transporter ATP binding subunit, 3.53; b0367 for taurine ABC transporter membrane subunit, 2.00; b0936 for aliphatic sulfonate ABC transporter periplasmic binding protein, 2.71; b2422 for sulfate/thiosulfate ABC transporter ATP binding subunit, 2.84; b3917 for sulfate/thiosulfate ABC transporter periplasmic binding protein Sbp, 8.73 (Supplementary data Table S4). In 2013, transcriptome analysis during iron starvation revealed high induction of genes related to the sulfate and taurine ABC-type transport systems in *P. aeruginosa* (van Delden *et al.*, 2013). Although a general overlap between iron starvation and sulfur sources is unclear, we propose two possibilities. The first is the uptake of taurine to supply iron. It was reported that taurine forms complexes with free metal ions such as iron or copper, and could work as a chelator (Trachtman *et al.*, 1992; Devi *et al.*, 2009). If complexes between taurine and iron are formed in the surrounding environment, bacteria will be able to obtain additional iron sources through their introduction. The second is that this is a programmed mechanism in response to increased demand for the cofactor. As already mentioned, the iron-chelating function of tropolone disabled nitrogen metabolism by cofactor deficiency (Fig. 5B). Because of cofactor form of iron sulfur compounds, bacteria may have misrecognized the lack of sulfur as well as iron, and subsequently induced their uptake systems.

### Integrative network to identify hub genes under phytotoxin conditions

In order to clarify high confidence hub genes, we entered the co-up-regulated DEGs from both toxoflavin and tropolone conditions (Fig. 6) into the STRING database (Szklarczyk *et al.*, 2017). As highly interconnected hub genes play important roles in biological systems (Liu *et al.*, 2016), genes were ranked by the degree of interactions among co-up-regulated DEGs. Finally, we identified five genes with more than nine interactions as hub genes (Fig. 6). The following five hub genes showed significant high expression in both two phytotoxins: b0585 for enterobactin esterase, 3.10 and 3.03 $\log_2$-fold change in toxoflavin and tropolone, respectively; b4511 for enterobactin biosynthesis protein YbdZ, 1.48 and 2.64; b1495 for putative TonB-dependent receptor, 1.22 and 2.02; b1705 for PF10636 family protein YdiE, 2.30 and 1.60; b2673 for glutaredoxin-like protein, 4.81 and 4.43 (Table 4). We noted that most hubs are closely involved in stress conditions derived from the two phytotoxins. To obtain sufficient iron, siderophore enterobactin production is the most efficient iron scavenging mechanism in members of the *Enterobacteriaceae* family (Raymond *et al.*, 2003). In addition to b4511 that directly produces enterobactin, b1495 (*tonB* gene) recognizes and imports enterobactin from outside the cells, and b0585 is responsible for removing iron ions from enterobactin for metabolic utilization (Langman *et al.*, 1972; Raymond *et al.*, 2003; Miethke and Marahiel, 2007). In other words, these hubs represent a major countermeasure for overcoming iron starvation by tropolone. On the other hand, enterobactin can be considered a crucial mechanism for dealing seby toxoflavin. To date, many studies have been reported that siderophore synthesis in microorganisms is controlled by oxidative stress in addition to iron availability (Cornish and Page, 1998; Tindale *et al.*, 2000; Lee *et al.*, 2011). *E. coli* produces higher amounts of enterobactin in culture conditions with increased oxidative stress for colony development (Peralta *et al.*, 2016). Interestingly, Adler *et al.* (Peralta *et al.*, 2016) demonstrated that after the release of iron ions, the linearized enterobactin molecule has three catechol moieties with the potential to stabilize ROS. In addition to enterobactin-related genes, b1705 (PF10636 family protein YdiE) and b2673 (glutaredoxin-like protein) genes can also play an important role in the utilization of iron ions. As a

**Table 4.** Function and expression of hub genes of co-up-regulated DEGs

| Gene | Function | Interactions[a] | $\log_2$ (Phytotoxin/Control) | |
|---|---|---|---|---|
| | | | Toxoflavin | Tropolone |
| b0585 | Enterochelin esterase | 10 | 3.10 | 3.03 |
| b4511 | Enterobactin biosynthesis protein YbdZ | 9 | 1.48 | 2.64 |
| b1495 | Putative TonB-dependent receptor | 9 | 1.22 | 2.02 |
| b1705 | PF10636 family protein YdiE | 9 | 2.30 | 1.60 |
| b2673 | Glutaredoxin-like protein | 9 | 4.81 | 4.43 |

[a] The number of interactions with other genes.

homologue of YdiE, the HemP protein of *B. multivorans* activates expression of a set of genes related to uptake of iron source hemin (McHugh *et al.*, 2003; Sato *et al.*, 2017). It was reported that the production of glutaredoxin, which delivers iron ions to enzymes on demand, is highly elevated upon iron starvation in *E. coli* (Fernandes *et al.*, 2005; Rouhier *et al.*, 2008). Thus, the hub genes obtained from network analysis indicated that they are located at a key intersection in the oxidative stress and iron starvation caused by toxoflavin and tropolone. Furthermore, the fact that these hubs are commonly induced by representative phytotoxins from *Burkholderia* species will be valuable information for subsequent applications for the detection and defense against these major virulence factor.

## Conclusion

In summary, we present, for the first time, an extensive analysis of the transcriptome of *E. coli* K-12 MG1655 in response to toxoflavin and tropolone exposure. Our data described the details of the bacterial responses under stress conditions caused by the two phytotoxins that had only been known in the literature. As the ROS due to toxoflavin were added to the bacteria, down-regulated DEGs showed the damage reaction cascade: ROS damage → bacterial membrane → diverse metabolism → oxidative phosphorylation or TCA cycle → energy breakdown → ribosome organization. Under iron starvation by tropolone, the disability of nitrogen metabolism using iron ions as cofactor would also have a critical effect on the inhibition of bacterial growth. On the other hand, under these harsh conditions, bacteria included countermeasure strategies against phytotoxins based on up-regulated DEGs. The up-regulated DEGs induced by toxoflavin exhibited flagellar structure and biofilms formation for evasion and protection, while tropolone increased the expression of genes associated with sulfate/taurine/alkanesulfonate transporters in sulfur metabolism. In addition, we have noted that some hub genes induced by both toxoflavin and tropolone focus on the enterobactin siderophore, which can function in both iron acquisition and reducing oxidative stress. The proposed models and interesting genes may facilitate future studies of physiological mechanisms underlying phytotoxin stresses in bacteria.

## Acknowledgements

This study was financially supported by the '2018 Post-Doc. Development Program' of Pusan National University. This research was supported by grants from the Strategic Initiative for Microbiomes in Agriculture and Food, Ministry of Agriculture, Food and Rural Affairs, Republic of Korea (No. 916009021SB010).

## Conflict of Interest

The authors declare that they have no conflict of interest.

## References

**Allen, A.E., Laroche, J., Maheswari, U., Lommer, M., Schauer, N., Lopez, P.J., Finazzi, G., Fernie, A.R., and Bowler, C.** 2008. Whole-cell response of the pennate diatom *Phaeodactylum tricornutum* to iron starvation. *Proc. Natl. Acad. Sci. USA* **105**, 10438–10443.

**Amina, M. and Ahmed, B.** 2017. *Pseudomonas* motility and antibiotics resistance. *J. Bioeng. Biomed. Sci.* **7**, 220.

**Antoniou, A., Tsolakidou, M.D., Stringlis, I.A., and Pantelides, I.S.** 2017. Rhizosphere microbiome recruited from a suppressive compost improves plant fitness and increases protection against vascular wilt pathogens of tomato. *Front. Plant Sci.* **8**, 2022.

**Azegami, K., Nishiyama, K., and Kato, H.** 1988. Effect of iron limitation on "*Pseudomonas plantarii*" growth and tropolone and protein production. *Appl. Environ. Microbiol.* **54**, 844–847.

**Azegami, K., Nishiyama, K., Watanabe, Y., Kadota, I., Ohuchi, A., and Fukazawa, C.** 1987. *Pseudomonas plantarii* sp. nov., the causal agent of rice seedling blight. *Int. J. Syst. Evol. Microbiol.* **37**, 144–152.

**Baldi, D.L., Higginson, E.E., Hocking, D.M., Praszkier, J., Cavaliere, R., James, C.E., Bennett Wood, V., Azzopardi, K.I., Turnbull, L., Lithgow, T., *et al.*** 2012. The type II secretion system and its ubiquitous lipoprotein substrate, SslE, are required for biofilm formation and virulence of enteropathogenic *Escherichia coli*. *Infect. Immun.* **80**, 2042–2052.

**Benjamini, Y. and Hochberg, Y.** 1995. Controlling the false discovery rate: a practical and powerful approach to multiple testing. *J. R. Stat. Soc. Ser. B.* **57**, 289–300.

**Benov, L. and Fridovich, I.** 1996. *Escherichia coli* exhibits negative chemotaxis in gradients of hydrogen peroxide, hypochlorite, and *N*-chlorotaurine: products of the respiratory burst of phagocytic cells. *Proc. Natl. Acad. Sci. USA* **93**, 4999–5002.

**Bentley, R.** 2008. A fresh look at natural tropolonoids. *Nat. Prod. Rep.* **25**, 118–138.

**Bischoff, V., Cookson, S.J., Wu, S., and Scheible, W.R.** 2009. Thaxtomin A affects CESA-complex density, expression of cell wall genes, cell wall composition, and causes ectopic lignification in *Arabidopsis thaliana* seedlings. *J. Exp. Bot.* **60**, 955–965.

**Blattner, F.R., Plunkett, G., Bloch, C., Perna, N., Burland, V., Riley, M., Collado Vides, J., Glasner, J., Rode, C., Mayhew, G., *et al.*** 1997. The complete genome sequence of *Escherichia coli* K-12. *Science* **277**, 1453–1462.

**Blount, Z.D.** 2015. The unexhausted potential of *E. coli*. *Elife* **4**, e05826.

**Blumwald, E.** 2000. Sodium transport and salt tolerance in plants. *Curr. Opin. Cell Biol.* **12**, 431–434.

**Brini, F. and Masmoudi, K.** 2012. Ion transporters and abiotic stress tolerance in plants. *ISRN Mol. Biol.* **2012**, 927436.

**Buchfink, B., Xie, C., and Huson, D.H.** 2015. Fast and sensitive protein alignment using DIAMOND. *Nat. Methods* **12**, 59–60.

**Champion, M.M., Campbell, C.S., Siegele, D.A., Russell, D.H., and Hu, J.C.** 2003. Proteome analysis of *Escherichia coli* K-12 by two-dimensional native-state chromatography and MALDI-MS. *Mol. Microbiol.* **47**, 383–396.

**Choi, O., Lee, Y., Han, I., Kim, H., Goo, E., Kim, J., and Hwang, I.** 2013. A simple and sensitive biosensor strain for detecting toxoflavin using β-galactosidase activity. *Biosens. Bioelectron.* **50**, 256–261.

**Choi, S.Y., Park, B., Choi, I.G., Sim, S.J., Lee, S.M., Um, Y., and Woo, H.M.** 2016. Transcriptome landscape of *Synechococcus elongatus* PCC 7942 for nitrogen starvation responses using RNA-seq. *Sci. Rep.* **6**, 30584.

**Chun, H., Choi, O., Goo, E., Kim, N., Kim, H., Kang, Y., Kim, J., Moon, J.S., and Hwang, I.** 2009. The quorum sensing-dependent gene *katG* of *Burkholderia glumae* is important for protection

from visible light. *J. Bacteriol.* **191**, 4152–4157.
**Coenye, T. and Vandamme, P.** 2003. Diversity and significance of *Burkholderia* species occupying diverse ecological niches. *Environ. Microbiol.* **5**, 719–729.
**Cornish, A.S. and Page, W.J.** 1998. The catecholate siderophores of *Azotobacter vinelandii*: their affinity for iron and role in oxygen stress management. *Microbiology* **144**, 1747–1754.
**Delcour, A.H.** 2009. Outer membrane permeability and antibiotic resistance. *Biochim. Biophys. Acta* **1794**, 808–816.
**Devi, S.L., Viswanathan, P., and Anuradha, C.** 2009. Taurine enhances the metabolism and detoxification of ethanol and prevents hepatic fibrosis in rats treated with iron and alcohol. *Environ. Toxicol. Pharmacol.* **27**, 120–126.
**Dröge, W.** 2002. Free radicals in the physiological control of cell function. *Physiol. Rev.* **82**, 47–95.
**Durbin, R.** 1991. Bacterial phytotoxins: mechanisms of action. *Experientia* **47**, 776–783.
**Eberl, L. and Vandamme, P.** 2016. Members of the genus *Burkholderia*: good and bad guys. *F1000Research* **5**, 1007.
**Ewing, B. and Green, P.** 1998. Base-calling of automated sequencer traces using phred. II. Error probabilities. *Genome Res.* **8**, 186–194.
**Farr, S.B. and Kogoma, T.** 1991. Oxidative stress responses in *Escherichia coli* and *Salmonella typhimurium*. *Microbiol. Rev.* **55**, 561–585.
**Fathima, A. and Rao, J.R.** 2018. Is Cr(III) toxic to bacteria: toxicity studies using *Bacillus subtilis* and *Escherichia coli* as model organism. *Arch. Microbiol.* **200**, 453–462.
**Fernandes, A.P., Fladvad, M., Berndt, C., Andrésen, C., Lillig, C.H., Neubauer, P., Sunnerhagen, M., Holmgren, A., and Vlamis-Gardikas, A.** 2005. A novel monothiol glutaredoxin (Grx4) from *Escherichia coli* can serve as a substrate for thioredoxin reductase. *J. Biol. Chem.* **280**, 24544–24552.
**Ferreira, A.S., Leitão, J.H., Silva, I.N., Pinheiro, P.F., Sousa, S.A., Ramos, C.G., and Moreira, L.M.** 2010. Distribution of cepacian biosynthesis genes among environmental and clinical *Burkholderia* strains and role of cepacian exopolysaccharide in resistance to stress conditions. *Appl. Environ. Microbiol.* **76**, 441–450.
**Franchini, A.G. and Egli, T.** 2006. Global gene expression in *Escherichia coli* K-12 during short-term and long-term adaptation to glucose-limited continuous culture conditions. *Microbiology* **152**, 2111–2127.
**Fry, B. and Loria, R.** 2002. Thaxtomin A: evidence for a plant cell wall target. *Physiol. Mol. Plant Pathol.* **60**, 1–8.
**Galperin, M.Y., Makarova, K.S., Wolf, Y.I., and Koonin, E.** 2015. Expanded microbial genome coverage and improved protein family annotation in the COG database. *Nucleic Acids Res.* **43**, D261–D269.
**Gooderham, W.J. and Hancock, R.E.** 2009. Regulation of virulence and antibiotic resistance by two-component regulatory systems in *Pseudomonas aeruginosa*. *FEMS Microbiol. Rev.* **33**, 279–294.
**Haas, B.J., Chin, M., Nusbaum, C., Birren, B.W., and Livny, J.** 2012. How deep is deep enough for RNA-Seq profiling of bacterial transcriptomes? *BMC Genomics* **13**, 734.
**Ham, J.H., Melanson, R.A., and Rush, M.C.** 2011. *Burkholderia glumae*: next major pathogen of rice? *Mol. Plant Pathol.* **12**, 329–339.
**Heiser, I., Oßwald, W., and Elstner, E.** 1998. The formation of reactive oxygen species by fungal and bacterial phytotoxins. *Plant Physiol.* **36**, 703–713.
**Hoch, J.A.** 2000. Two-component and phosphorelay signal transduction. *Curr. Opin. Microbiol.* **3**, 165–170.
**Hogenhout, S.A., Van der Hoorn, R.A.L., Terauchi, R., and Kamoun, S.** 2009. Emerging concepts in effector biology of plant-associated organisms. *Mol. Plant Microbe Interact.* **22**, 115–122.
**Hu, J.C., Sherlock, G., Siegele, D.A., Aleksander, S.A., Ball, C.A., Demeter, J., Gouni, S., Holland, T.A., Karp, P.D., Lewis, J.E., *et al.*** 2014. PortEco: a resource for exploring bacterial biology through high-throughput data and analysis tools. *Nucleic Acids Res.* **42**, D677–D684.
**Ieva, R.** 2017. Interfering with outer membrane biogenesis to fight Gram-negative bacterial pathogens. *Virulence* **8**, 1049–1052.
**Jacobs, J.M., Babujee, L., Meng, F., Milling, A., and Allen, C.** 2012. The *in planta* transcriptome of *Ralstonia solanacearum*: conserved physiological and virulence strategies during bacterial wilt of tomato. *MBio* **3**, e00114-12.
**Jeong, Y., Kim, J., Kim, S., Kang, Y., Nagamatsu, T., and Hwang, I.** 2003. Toxoflavin produced by *Burkholderia glumae* causing rice grain rot is responsible for inducing bacterial wilt in many field crops. *Plant Dis.* **87**, 890–895.
**Jing, X., Mi, T., Zhen, Y., Wang, H., and Yu, Z.** 2019. Influence of N, P, Fe nutrients availability on nitrogen metabolism-relevant genes expression in *Skeletonema marinoi*. *J. Ocean Univ. China* **18**, 239–252.
**Jung, B., Park, J., Kim, N., Li, T., Kim, S., Bartley, L.E., Kim, J., Kim, I., Kang, Y., Yun, K., *et al.*** 2018. Cooperative interactions between seed-borne bacterial and air-borne fungal pathogens on rice. *Nat. Commun.* **9**, 31.
**Kashef, N. and Hamblin, M.R.** 2017. Can microbial cells develop resistance to oxidative stress in antimicrobial photodynamic inactivation? *Drug Resist. Updat.* **31**, 31–42.
**Keseler, I.M., Mackie, A., Peralta Gil, M., Santos Zavaleta, A., Gama Castro, S., Bonavides Martínez, C., Fulcher, C., Huerta, A.M., Kothari, A., Krummenacker, M., *et al.*** 2013. EcoCyc: fusing model organism databases with systems biology. *Nucleic Acids Res.* **41**, D605–D612.
**Kim, J., Kang, Y., Choi, O., Jeong, Y., Jeong, J.E., Lim, J.Y., Kim, M., Moon, J.S., Suga, H., and Hwang, I.** 2007. Regulation of polar flagellum genes is mediated by quorum sensing and FlhDC in *Burkholderia glumae*. *Mol. Microbiol.* **64**, 165–179.
**Kim, J., Kim, J.G., Kang, Y., Jang, J.Y., Jog, G.J., Lim, J.Y., Kim, S., Suga, H., Nagamatsu, T., and Hwang, I.** 2004. Quorum sensing and the LysR-type transcriptional activator ToxR regulate toxoflavin biosynthesis and transport in *Burkholderia glumae*. *Mol. Microbiol.* **54**, 921–934.
**Kim, S., Park, J., Kim, J.H., Lee, J., Bang, B., Hwang, I., and Seo, Y.S.** 2013. RNAseq-based transcriptome analysis of *Burkholderia glumae* quorum sensing. *Plant Pathol. J.* **29**, 249–259.
**Kim, S., Park, J., Lee, J., Shin, D., Park, D.S., Lim, J.S., Choi, I.Y., and Seo, Y.S.** 2014. Understanding pathogenic *Burkholderia glumae* metabolic and signaling pathways within rice tissues through *in vivo* transcriptome analyses. *Gene* **547**, 77–85.
**Krämer, R.** 2010. Bacterial stimulus perception and signal transduction: response to osmotic stress. *Chem. Rec.* **10**, 217–229.
**Kuehn, M. and Kesty, N.** 2005. Bacterial outer membrane vesicles and the host-pathogen interaction. *Genes Dev.* **19**, 2645–2655.
**Langman, L., Young, I.G., Frost, G.E., Rosenberg, H., and Gibson, F.** 1972. Enterochelin system of iron transport in *Escherichia coli*: mutations affecting ferric-enterochelin esterase. *J. Bacteriol.* **112**, 1142–1149.
**Lareen, A., Burton, F., and Schäfer, P.** 2016. Plant root-microbe communication in shaping root microbiomes. *Plant Mol. Biol.* **90**, 575–587.
**Latuasan, H.E. and Berends, W.** 1961. On the origin of the toxicity of toxoflavin. *Biochim. Biophys. Acta* **52**, 502–508.
**Lee, J., Park, J., Kim, S., Park, I., and Seo, Y.S.** 2016. Differential regulation of toxoflavin production and its role in the enhanced virulence of *Burkholderia gladioli*. *Mol. Plant Pathol.* **17**, 65–76.
**Lee, J.Y., Passalacqua, K.D., Hanna, P.C., and Sherman, D.H.** 2011. Regulation of petrobactin and bacillibactin biosynthesis in *Bacillus anthracis* under iron and oxygen variation. *PLoS One* **6**, e20777.
**Li, H. and Durbin, R.** 2009. Fast and accurate short read alignment with Burrows-Wheeler transform. *Bioinformatics* **25**, 1754–1760.
**Li, H., Handsaker, B., Wysoker, A., Fennell, T., Ruan, J., Homer,**

**N., Marth, G., Abecasis, G., and Durbin, R.** 2009. The Sequence Alignment/Map (SAM) format and SAMtools. *Bioinformatics* **25**, 2078–2079.

**Liao, Y., Smyth, G.K., and Shi, W.** 2014. featureCounts: an efficient general purpose program for assigning sequence reads to genomic features. *Bioinformatics* **30**, 923–930.

**Liu, J., Jing, L., and Tu, X.** 2016. Weighted gene co-expression network analysis identifies specific modules and hub genes related to coronary artery disease. *BMC Cardiovasc. Disord.* **16**, 54.

**Liu, X., Shen, B., Du, P., Wang, N., Wang, J., Li, J., and Sun, A.** 2017. Transcriptomic analysis of the response of *Pseudomonas fluorescens* to epigallocatechin gallate by RNA-seq. *PLoS One* **12**, e0177938.

**Liu, B., Zhang, Y., and Zhang, W.** 2014. RNA-Seq-based analysis of cold shock response in *Thermoanaerobacter tengcongensis*, a bacterium harboring a single cold shock protein encoding gene. *PLoS One* **9**, e93289.

**Maathuis, F.J.** 2007. Monovalent cation transporters; establishing a link between bioinformatics and physiology. *Plant Soil* **301**, 1–15.

**McCloskey, D., Gangoiti, J.A., King, Z.A., Naviaux, R.K., Barshop, B.A., Palsson, B.O., and Feist, A.M.** 2014. A model-driven quantitative metabolomics analysis of aerobic and anaerobic metabolism in *E. coli* K-12 MG1655 that is biochemically and thermodynamically consistent. *Biotechnol. Bioeng.* **111**, 803–815.

**McHugh, J.P., Rodríguez-Quiñones, F., Abdul-Tehrani, H., Svistunenko, D.A., Poole, R.K., Cooper, C.E., and Andrews, S.C.** 2003. Global iron-dependent gene regulation in *Escherichia coli*. A new mechanism for iron homeostasis. *J. Biol. Chem.* **278**, 29478–29486.

**McIntosh, B.K., Renfro, D.P., Knapp, G.S., Lairikyengbam, C.R., Liles, N.M., Niu, L., Supak, A.M., Venkatraman, A., Zweifel, A.E., Siegele, D.A., *et al.*** 2012. EcoliWiki: a wiki-based community resource for *Escherichia coli*. *Nucleic Acids Res.* **40**, D1270–D1277.

**Miethke, M. and Marahiel, M.A.** 2007. Siderophore-based iron acquisition and pathogen control. *Microbiol. Mol. Biol. Rev.* **71**, 413–451.

**Miwa, S., Kihira, E., Yoshioka, A., Nakasone, K., Okamoto, S., Hatano, M., Igarashi, M., Eguchi, Y., Kato, A., Ichikawa, N., *et al.*** 2016. Identification of the three genes involved in controlling production of a phytotoxin tropolone in *Burkholderia plantarii*. *J. Bacteriol.* **198**, 1604–1609.

**Möbius, N. and Hertweck, C.** 2009. Fungal phytotoxins as mediators of virulence. *Curr. Opin. Plant Biol.* **12**, 390–398.

**Morozkina, E.V. and Zvyagilskaya, R.A.** 2007. Nitrate reductases: structure, functions, and effect of stress factors. *Biochemistry (Mosc).* **72**, 1151–1160.

**Mortazavi, A., Williams, B.A., McCue, K., Schaeffer, L., and Wold, B.** 2008. Mapping and quantifying mammalian transcriptomes by RNA-Seq. *Nat. Methods* **5**, 621–628.

**Nandakumar, R., Shahjahan, A.K.M., Yuan, X.L., Dickstein, E.R., Groth, D.E., Clark, C.A., Cartwright, R.D., and Rush, M.C.** 2009. *Burkholderia glumae* and *B. gladioli* cause bacterial panicle blight in rice in the southern United States. *Plant Dis.* **93**, 896–905.

**Parkinson, J.S. and Kofoid, E.C.** 1992. Communication modules in bacterial signaling proteins. *Annu. Rev. Genet.* **26**, 71–112.

**Peralta, D.R., Adler, C., Corbalán, N.S., Paz García, E.C., Pomares, M.F., and Vincent, P.A.** 2016. Enterobactin as part of the oxidative stress response repertoire. *PLoS One* **11**, e0157799.

**Phaniendra, A., Jestadi, D.B., and Periyasamy, L.** 2015. Free radicals: properties, sources, targets, and their implication in various diseases. *Indian J. Clin. Biochem.* **30**, 11–26.

**Qiao, Q., Wang, F., Zhang, J., Chen, Y., Zhang, C., Liu, G., Zhang, H., Ma, C., and Zhang, J.** 2017. The variation in the rhizosphere microbiome of cotton with soil type, genotype and developmental stage. *Sci. Rep.* **7**, 3940.

**Qureshi, R. and Sacan, A.** 2013. Weighted set enrichment of gene expression data. *BMC Syst. Biol.* **7**, S10.

**Raymond, K.N., Dertz, E.A., and Kim, S.S.** 2003. Enterobactin: an archetype for microbial iron transport. *Proc. Natl. Acad. Sci. USA* **100**, 3584–3588.

**Reitzer, L.J.** 1987. Ammonia assimilation and the biosynthesis of glutamine, glutamate, aspartate, asparagine, L-alanine and D-alanine. *In Escherichia coli and Salmonella typhimurium: Cellular and Molecular Biology* **2**, 302–320.

**Reitzer, L.** 2003. Nitrogen assimilation and global regulation in *Escherichia coli*. *Annu. Rev. Microbiol.* **57**, 155–176.

**Richardson, D., Vanwye, J., Exum, A., and Cowen, R.** 2007. High-throughput species identification: from DNA isolation to bioinformatics. *Mol. Ecol. Notes* **7**, 199–207.

**Riley, M., Abe, T., Arnaud, M.B., Berlyn, M.K.B., Blattner, F.R., Chaudhuri, R.R., Glasner, J.D., Horiuchi, T., Keseler, I.M., Kosuge, T., *et al.*** 2006. *Escherichia coli* K-12: a cooperatively developed annotation snapshot--2005. *Nucleic Acids Res.* **34**, 1–9.

**Robinson, M.D., McCarthy, D.J., and K, Smyth, G.** 2010. edgeR: a Bioconductor package for differential expression analysis of digital gene expression data. *Bioinformatics* **26**, 139–140.

**Robinson, M.D. and Smyth, G.K.** 2008. Small-sample estimation of negative binomial dispersion, with applications to SAGE data. *Biostatistics* **9**, 321–332.

**Rouhier, N., Lemaire, S.D., and Jacquot, J.P.** 2008. The role of glutathione in photosynthetic organisms: emerging functions for glutaredoxins and glutathionylation. *Annu. Rev. Plant Biol.* **59**, 143–166.

**Ruiz, N., Kahne, D., and Silhavy, T.J.** 2006. Advances in understanding bacterial outer-membrane biogenesis. *Nat. Rev. Microbiol.* **4**, 57–66.

**Sato, T., Nonoyama, S., Kimura, A., Nagata, Y., Ohtsubo, Y., and Tsuda, M.** 2017. The small protein HemP is a transcriptional activator for the hemin uptake operon in *Burkholderia multivorans* ATCC 17616. *Appl. Environ. Microbiol.* **83**, e00479-17.

**Simon, J., Sänger, M., Schuster, S.C., and Gross, R.** 2003. Electron transport to periplasmic nitrate reductase (NapA) of *Wolinella succinogenes* is independent of a NapC protein. *Mol. Microbiol.* **49**, 69–79.

**Solis, R., Bertani, I., Degrassi, G., Devescovi, G., and Venturi, V.** 2006. Involvement of quorum sensing and RpoS in rice seedling blight caused by *Burkholderia plantarii*. *FEMS Microbiol. Lett.* **259**, 106–112.

**Suzuki, F., Zhu, Y., Sawada, H., and Matsuda, I.** 1998. Identification of proteins involved in toxin production by *Pseudomonas glumae*. *Japanese J. Phytopathol.* **64**, 75–79.

**Szklarczyk, D., Morris, J.H., Cook, H., Kuhn, M., Wyder, S., Simonovic, M., Santos, A., Doncheva, N.T., Roth, A., Bork, P., *et al.*** 2017. The STRING database in 2017: quality-controlled protein–protein association networks, made broadly accessible. *Nucleic Acids Res.* **45**, D362–D368.

**Timmermans, K.R., Stolte, W., and de Baar, H.J.W.** 1994. Iron-mediated effects on nitrate reductase in marine phytoplankton. *Mar. Biol.* **121**, 389–396.

**Tindale, A.E., Mehrotra, M., Ottem, D., and Page, W.J.** 2000. Dual regulation of catecholate siderophore biosynthesis in *Azotobacter vinelandii* by iron and oxidative stress. *Microbiology* **146**, 1617–1626.

**Trachtman, H., Del Pizzo, R., Futterweit, S., Levine, D., Rao, P.S., Valderrama, E., and Sturman, J.A.** 1992. Taurine attenuates renal disease in chronic puromycin aminonucleoside nephropathy. *Am. J. Physiol. Physiol.* **262**, F117–F123.

**Trust, T.J.** 1975. Antibacterial activity of tropolone. *Antimicrob. Agents Chemother.* **7**, 500–506.

**Ugurlu, A., Yagci, A., Ulusoy, S., and Aksu, B.** 2016. Phenolic compounds affect production of pyocyanin, swarming motility and biofilm formation of *Pseudomonas aeruginosa*. *Asian Pac. J.*

*Trop. Biomed.* **6**, 698–701.

**Ura, H., Furuya, N., Iiyama, K., Hidaka, M., Tsuchiya, K., and Matsuyama, N.** 2006. *Burkholderia gladioli* associated with symptoms of bacterial grain rot and leaf-sheath browning of rice plants. *J. Gen. Plant Pathol.* **72**, 98–103.

**van Delden, C., Page, M., and Köhler, T.** 2013. Involvement of Fe uptake systems and AmpC β-lactamase in susceptibility to the siderophore monosulfactam BAL30072 in *Pseudomonas aeruginosa*. *Antimicrob. Agents Chemother.* **57**, 2095–2102.

**Vasudevan, R.** 2014. Biofilms: microbial cities of scientific significance. *J. Microbiol. Exp.* **1**, 00014.

**Wakimoto, S., Hirayae, K., Tsuchiya, K., Kushima, Y., Furuya, N., and Matsuyama, N.** 1986. Production of antibiotics by plant pathogenic pseudomonads. *Japanese J. Phytopathol.* **52,** 835–842.

**Wang, M., Hashimoto, M., and Hashidoko, Y.** 2013. Repression of tropolone production and induction of a *Burkholderia plantarii* pseudo-biofilm by carot-4-en-9,10-diol, a cell-to-cell signaling disrupter produced by *Trichoderma virens*. *PLoS One* **8**, e78024.

**Wang, M., Wei, P., Cao, M., Zhu, L., and Lu, Y.** 2016. First report of rice seedling blight caused by *Burkholderia plantarii* in North and Southeast China. *Plant Dis.* **100**, 645.

**Willi, J., Küpfer, P., Evéquoz, D., Fernandez, G., Katz, A., Leumann, C., and Polacek, N.** 2018. Oxidative stress damages rRNA inside the ribosome and differentially affects the catalytic center. *Nucleic Acids Res.* **46**, 1945–1957.

**Williams, L.D., Glenn, A.E., Zimeri, A.M., Bacon, C.W., Smith, M.A., and Riley, R.T.** 2007. Fumonisin disruption of ceramide biosynthesis in maize roots and the effects on plant development and *Fusarium verticillioides*-induced seedling disease. *J. Agric. Food Chem.* **55**, 2937–2946.

**Yang, X.Y., Sun, B., Zhang, L., Li, N., Han, J., Zhang, J., Sun, X., and He, Q.Y.** 2014. Chemical interference with iron transport systems to suppress bacterial growth of *Streptococcus pneumoniae*. *PLoS One* **9**, e105953.

**Yoneyama, K., Kono, Y., Yamaguchi, I., Horikoshi, M., and Hirooka, T.** 1998. Toxoflavin is an essential factor for virulence of *Burkholderia glumae* causing rice seedling rot disease. *Japanese J. Phytopathol.* **64**, 91–96.

**Zhou, J., Richardson, A.J., and Rudd, K.E.** 2013. EcoGene-RefSeq: EcoGene tools applied to the RefSeq prokaryotic genomes. *Bioinformatics* **29**, 1917–1918.